

## Article

# PNP-Ligated Rare-Earth Metal Catalysts for Efficient Polymerization of Isoprene

Rongqing Ma <sup>1</sup>, Hongfan Hu <sup>2</sup>, Xinle Li <sup>2</sup>, Yi Zhou <sup>2</sup>, Huashu Li <sup>2</sup>, Xin Sun <sup>2</sup>, Xueqin Zhang <sup>2</sup>, Guoliang Mao <sup>1</sup> and Shixuan Xin <sup>1,2,\*</sup>

<sup>1</sup> Provincial Key Laboratory of Polyolefin New Materials, College of Chemical Engineering, Northeast Petroleum University, Daqing 163318, China

<sup>2</sup> PetroChina Petrochemical Research Institute, 7 Kunlun Road, Changping District, Beijing 102206, China

\* Correspondence: xinshixuan@petrochina.com.cn; Tel.: +86-10-80165612 or +86-186-10096542

**Abstract:** The tridentate PNP ligand-supported rare-earth metal complexes, i.e., bis[*o*-diphenylphosphinophenyl]amido-Re-bis[*o*-dimethylaminobenzyl], [(Ph<sub>2</sub>P-*o*-C<sub>6</sub>H<sub>4</sub>)<sub>2</sub>N]Re[(CH<sub>2</sub>-*o*-Me<sub>2</sub>N(C<sub>6</sub>H<sub>4</sub>))<sub>2</sub>] (Re = Y, **1**; Nd, **2**; Gd, **3**) were applied to isoprene polymerization. When activated with borate activator ([PhMe<sub>2</sub>NH][B(C<sub>6</sub>F<sub>5</sub>)<sub>4</sub>] (NH-BARF), catalysts **1** and **3** exhibited excellent catalytic efficiency in aromatic media, produced very-high to ultrahigh molecular weight (M<sub>w</sub> over 130 × 10<sup>4</sup> g/mol) polyisoprene rubber (PIR), and the obtained PIR contained over 98% *cis*-1,4 head-to-tail repeating unites. In most cases, the borate-activated polymerization reaction proceeded in a quasi-living pattern (PDI = 1.2–1.5) under controlled monomer conversion; whereas, activated with the commercially available modified methylaluminoxane (MMAO3A) in aliphatic hydrocarbon media, complexes **1**, **2** and **3** all showed high catalytic efficiency, produced high molecular weight PIR with narrow molecular weight distribution (PDI ≤ 2.0) and high *cis*-1,4 head-to tail repeating unites in the range of 91–95%. Thus, the catalyst systems that consisted of **1**, **2** and **3**/MMAO3A, are closely relevant to the current industrial polybutadiene rubber (PBR) and PIR production processes.

**Keywords:** polyisoprene; rare-earth metal; polymerization; catalyst; elastomer; natural rubber



**Citation:** Ma, R.; Hu, H.; Li, X.; Zhou, Y.; Li, H.; Sun, X.; Zhang, X.; Mao, G.; Xin, S. PNP-Ligated Rare-Earth Metal Catalysts for Efficient Polymerization of Isoprene. *Catalysts* **2022**, *12*, 1131. <https://doi.org/10.3390/catal12101131>

Academic Editors: Adriano G. Fisch and Yue Yu

Received: 31 July 2022

Accepted: 31 August 2022

Published: 28 September 2022

**Publisher's Note:** MDPI stays neutral with regard to jurisdictional claims in published maps and institutional affiliations.



**Copyright:** © 2022 by the authors. Licensee MDPI, Basel, Switzerland. This article is an open access article distributed under the terms and conditions of the Creative Commons Attribution (CC BY) license (<https://creativecommons.org/licenses/by/4.0/>).

## 1. Introduction

Synthetic polyisoprene rubber (sPIR) was first prepared in 1879 by the polymerization of isoprene monomer derived from the destruction of natural rubber (NR), and the commercial products of sPIR were produced nearly 90 years later through the utilization of the Ziegler-type catalyst [1]. Nowadays, sPIR is one of the indispensable high-performance elastic materials used in various industrial applications, and the tire industry alone consumes around 60% sPIR.

The high stereoregularity and high molecular weight of natural rubber (NR) molecules endow the vulcanized NR material unique physical properties, such as low thermogenesis, low rolling resistance, high tear and abrasion resistance, etc. Therefore, the sPIR industry practiced various ways to mimic the NR molecular microstructure and properties [2–7]; the long-term unremitting efforts reward the rubber industry with significant physical property improvement on sPIR materials. However, in order to regulate the sPIR structure and properties matching the NR, precise control of isoprene monomer stereoregularity and connectivity in the polymer chain remain great challenges to academic and industrial researchers.

In an sPIR macromolecule, isoprene monomer can adapt several stereoregularity and connectivity modes, for example the *cis*-1,4 and *trans*-1,4 connectivity appeared in two types of natural rubbers referred to as cNR (*Hevea brasiliensis*) and tNR (balata, from bully tree or *Manilkara bidentata*), while the sPIR made from different catalytic systems may produce several types of sPIR microstructures [8–11], such as highly *cis*-1,4 PIR (cPIR) and highly

*trans*-1,4 PIR (*t*PIR) with head-to-head and tail-to-tail connection, or special regioselective macromolecules with 3,4-connectivity mode to give *isotactic*-3,4 (*i*PI34), *syndiotactic*-3,4 (*s*PI34) and *atactic*-3,4 (*a*PI34) macromolecules, which appear as crystalline or amorphous depending on the stereoregularity level of the macromolecules. Although 1,2-connectivity is a mode that has appeared in some isoprene macromolecules, polymers with predominant 1,2-connectivity are rare.

sPIR are used in tires, footwear, hoses, belts, foamed products and medical accessories (including medial gloves, balloons). Medical applications are experiencing a fast increase in demand [12,13]. Thus, through sPIR microstructural control to replicate cNR's molecular and physical characteristics is the apex, and empirically, both the catalyst structure and the polymerization process modifications are the most efficient approaches. The discovery of rare-earth metals as high-performance catalysts for the polymerization of conjugated dienes has significantly advanced the sPIR microstructure control toward the ultimate goals [13–19].

In this work, the tridentate PNP molecule, bis(*o*-diphenylphosphinophenyl)amine [*o*-Ph<sub>2</sub>P(C<sub>6</sub>H<sub>4</sub>)<sub>2</sub>NH], coordinated rare-earth metal (Y, Nd, Gd) complexes, bis[*o*-diphenylphosphinophenyl]amido-Re-bis[*o*-dimethylaminobenzyl], [(Ph<sub>2</sub>P-*o*-C<sub>6</sub>H<sub>4</sub>)<sub>2</sub>N]Re[(CH<sub>2</sub>-*o*-Me<sub>2</sub>N(C<sub>6</sub>H<sub>4</sub>))<sub>2</sub>]: (Re = Y, **1**; Nd, **2**; Gd, **3**), combined with either borate activator [(PhMe<sub>2</sub>NH)B(C<sub>6</sub>F<sub>5</sub>)<sub>4</sub>] (NH-BARF) in aromatic media, or mixed with commercial MMAO3A in aliphatic hydrocarbons, are utilized to isoprene homopolymerization. The **1**-NH-BARF and **3**-NH-BARF catalytic systems exhibit excellent catalytic efficiency and stereoselectivity in toluene and produce very-high to ultrahigh molecular weight ( $M_w \geq 130 \times 10^4$  g/mol) sPIR, containing over 98% *cis*-1,4 head-to-tail repeating isoprene units, while **2**-NH-BARF showed marginal activity towards isoprene polymerization. Moreover, under controlled monomer conversion, the borate-activated polymerization reaction proceeded in a quasi-living pattern (PDI = 1.2–1.5). When complexes activated with MMAO3A in aliphatic hydrocarbon, **1**–**3**/MMAO3A catalyst systems showed high catalytic efficiency, produced high molecular weight PIR with narrow molecular weight distribution (PDI  $\leq$  2.0) and high *cis*-1,4 head-to tail repeating isoprene unites in the range of 91–95%. Thus, the catalyst systems that consisted of **1**, **2** and **3**/MMAO3A are highly relevant to the current industrial *cis*-polybutadiene rubber (cPBR) and cPIR production processes.

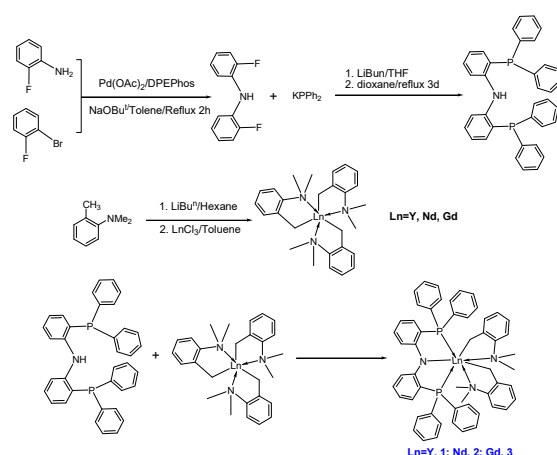
In comparison to the currently adapted Nd/aliphatic acid/AlR<sub>3</sub> multi-component catalytic system, the **1**–**3**/NH-MMAO3A catalytic systems generate high molecular weight cPIR and especially high productivity, certainly encouraging the rubber industry to further create diverse production processes for advance sPIR materials.

Thus, this study provided a paradigm of an aliphatic hydrocarbon soluble cationic rare-earth metal catalyst system, for the synthetic rubber industry to develop a 'drop-in' high performance catalyst system using the current facility and processes, ultimately for the production of new sPIR and/or sPBR products.

## 2. Results

### 2.1. Preparation of the Tridentate PNP-Ligated Rare-Earth Metal Complexes

The neutral tridentate ligand [*o*-Ph<sub>2</sub>P(C<sub>6</sub>H<sub>4</sub>)<sub>2</sub>NH] (PNP ligand) and the PNP co-ordinated rare-earth metal complexes bis[*o*-diphenylphosphinophenyl]amido-Re-bis[*o*-dimethylaminobenzyl], [(Ph<sub>2</sub>P-*o*-C<sub>6</sub>H<sub>4</sub>)<sub>2</sub>N]Re[(CH<sub>2</sub>-*o*-Me<sub>2</sub>N(C<sub>6</sub>H<sub>4</sub>))<sub>2</sub>]: (Re = Y, **1**; Nd, **2**; Gd, **3**), were prepared according to modified literature methods (Scheme 1) [20].



**Scheme 1.** Synthesis of the neutral rare-earth metal complexes bearing one tridentate bis[*o*-diphenylphosphinophenyl]amido (PNP) and two *o*-dimethylaminobenzyl (*o*-Me<sub>2</sub>N-Bz) ligands.

In a modified synthetic procedure, the deprotonation of the bis(2-Fluorophenyl)amine with organolithium or alkaline metal hydride prior to adding the freshly prepared KPPH<sub>2</sub> can substantially increase the yield of the tridentate PNP ligand, and overall yields of 86% for complexes **1–3** can be achieved. In this work, tris(*o*-dimethylaminobenzyl)rare-earth metal intermediate [Me<sub>2</sub>N-*o*-(C<sub>6</sub>H<sub>4</sub>)CH<sub>2</sub>-]<sub>3</sub>Re (Re = Y, Nd, Gd) were used, and the resulting complexes **1–3** contained no additional nuclear-phallic solvent molecules in their coordination sphere [20]. The composition and structure of **1** was confirmed by the <sup>1</sup>H and <sup>31</sup>P NMR spectroscopy method. The composition and molecular parameters of paramagnetic analogs **2** and **3** were identified with elemental analysis and high-resolution mass spectroscopy (HR-MS). The <sup>1</sup>H and <sup>31</sup>P NMR spectrum of the Yttrium complex **1** are presented in Figure 1. The analytical data for complexes **2** and **3** are summarized in Section 4.

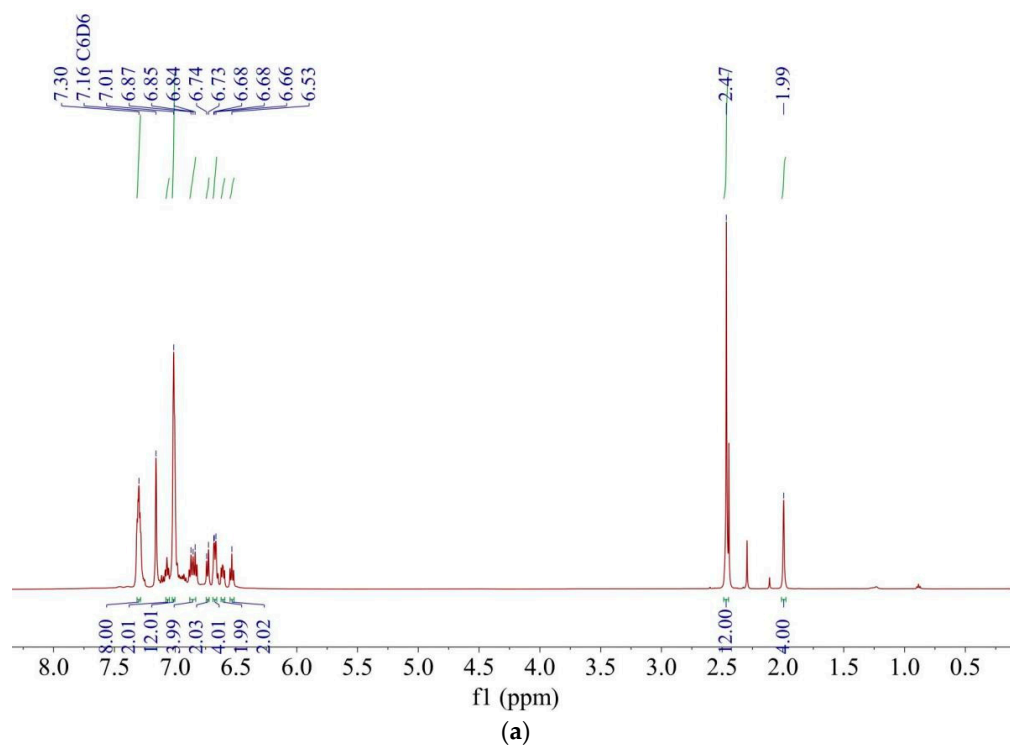


**Figure 1.** Cont.

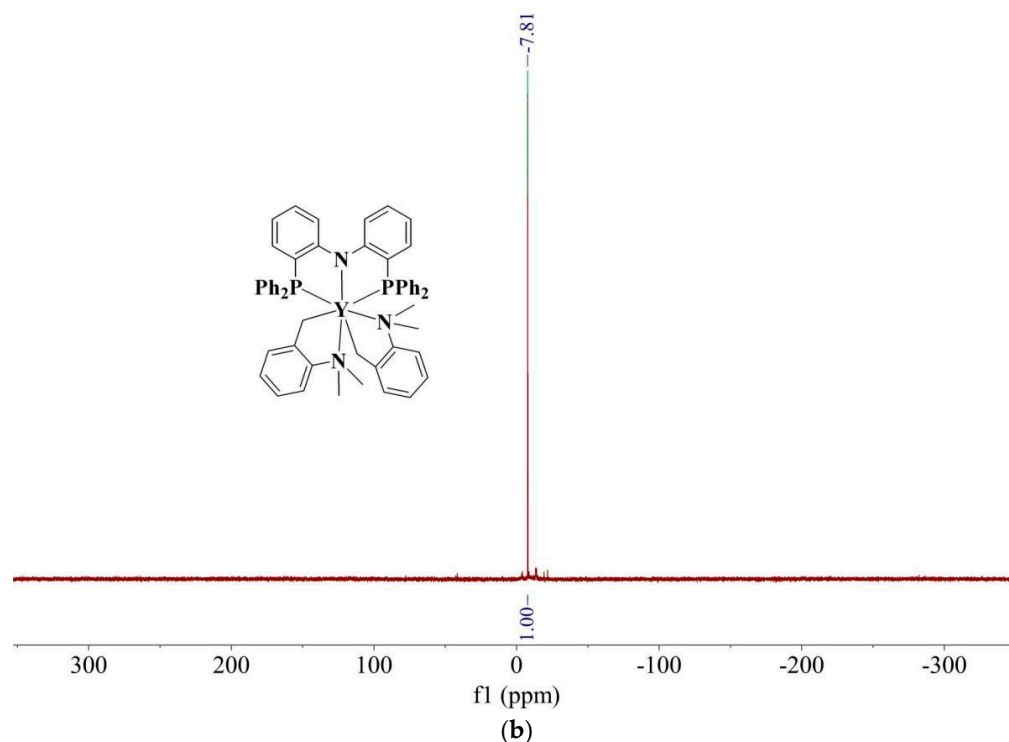


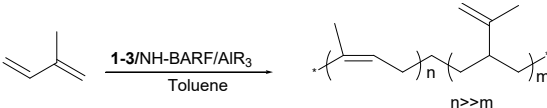
**Figure 1.**  $^1\text{H}$  and  $^{31}\text{P}$  NMR spectra of complex 1. (a) Proton NMR spectrum of complex 1; (b)  $^{31}\text{P}$  NMR spectrum of complex 1.

## 2.2. Polymerization of Isoprene with Borate [NH-BARF] Activator in Toluene

Currently, the familiar Ziegler-type rare-earth metal catalyst system, i.e., the slurry catalyst precursor derived from neodymium/alkylaluminum halide, is usually used for the production of *cis*-1,4 sPIR (*cis*-1,4 content around 96–99%) with relatively narrow molecular weight distribution (PDI~3–5). Owing to the Nd system's low efficiency, the long and sophisticate raw product deashing process is inevitable, and the catalyst aging-time affects causes unsustainable product quality control. Thus, the multiple undesirable factors certainly elevate the production cost [21]. On the other hand, frequently reported single-site rare-earth metal catalyst systems [16–19,22–28] usually exhibit high catalyst efficiency and high stereoselectivity, thus, encouraging the rubber industry to explore the opportunity of using these systems in the current sPIR processes.

A similar catalyst system consists of tridentate PNP-ligated rare-earth metal bis(trimethylsilylmethyl) complexes and NH-BARF activator, catalyzed isoprene in a living polymerization pattern (PDI ca. 1.1), with very high stereoselectivity (*cis*-1,4 content ca. 99%) and head-to-tail connectivity. [18] However, to ensure that the NH-BARF activator is soluble, the polymerization reaction is conducted in halogenated aromatic solvent, which is not adopted in rubber industries for economic and environmental reasons.

In our approach, the commonly used solvents toluene and hexane were tested. The polymerization results of 1–3/NH-BARF catalyst systems in toluene are summarized in Table 1. Several factors affecting the sPIR molecular weight and microstructures, and some interesting outcomes can be concluded (*vide infra*). Complex 2, that was activated with NH-BARF, showed, essentially, inactivity towards isoprene polymerization, and all three complexes activated with NH-BARF were silent in hexane toward isoprene polymerization—an obvious reason of insoluble cationic catalysts species in the media.

**Table 1.** Polymerization of isoprene (IP) with **1**, **2**, **3** and NH-BARF catalyst systems.


Run	Cat.	$P_t$ (min)	$T_p$ (°C)	Conversion %	$M_w^a$ (kg/mol)	PDI <sup>a</sup>	Microstructure <sup>b</sup>		Tg <sup>c</sup>
							<i>cis</i> -1,4%	3,4%	
1	<b>1</b>	5	20	93.6	777	1.54	(98.69)	1.31	
2	<b>2</b>	780	20	trace	—	—	—	—	—
3	<b>3</b>	5	20	100	369	1.28	(98.58)	1.42	—
4	<b>3</b>	30	0	78	282	1.27	98.63 (98.63)	1.37	
5	<b>3</b>	60	0	88	480	1.24	98.45 (98.63)	1.55	−72
6	<b>3</b>	60	0	92	440	1.32	98.44 (98.58)	1.56	—
7	<b>3</b>	90	0	99	376	1.39	98.51 (98.55)	1.49	—
8	<b>3</b>	120	0	100	387	1.29	98.78 (98.53)	1.22	—
9	<b>3</b>	2	20	52	368	1.30	98.66 (98.50)	1.34	—
10	<b>3</b>	2	40	92	468	1.27	98.44 (98.52)	1.56	—
11	<b>3</b>	2	60	99.5	452	1.43	98.30 (98.47)	1.70	—
12	<b>3</b>	2	80	100	476	1.32	98.60 (98.42)	1.40	—
13	<b>3</b> <sup>d</sup>	30	20	100	718	1.68	(98.64)	1.36	—
14	<b>3</b> <sup>e</sup>	30	20	100	836	1.57	(98.54)	1.46	—
15	<b>3</b> <sup>f</sup>	30	20	100	886	1.58	(98.65)	1.35	—
16	<b>3</b> <sup>g</sup>	30	20	90.2	1356	2.07	(98.67)	1.33	—
17	<b>3</b>	8	20	99	357	1.34	(98.56)	1.44	
18	<b>3</b>	10	20	100	348	1.18	98.66 (98.50)	1.34	−70
19	<b>3</b>	30	20	100	625	2.29	(98.64)	1.36	

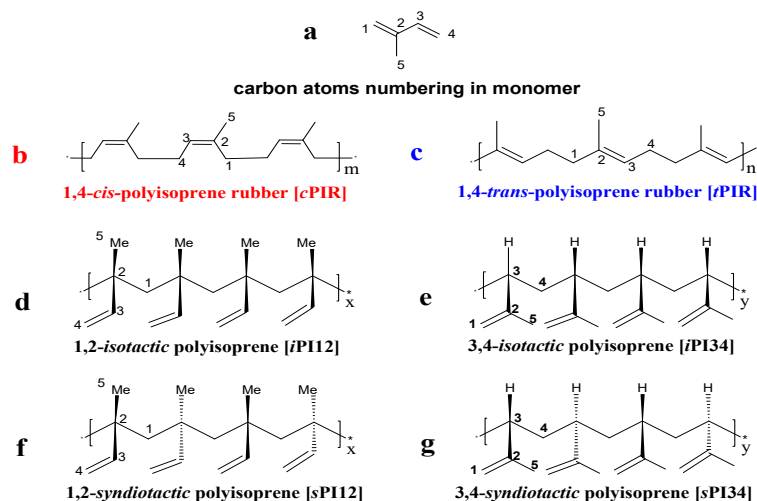
Polymerization conditions: IP 1.0 M toluene solution 10 mL (10 mM),  $AlBu^i_3$  50  $\mu$ M, Re 5.0  $\mu$ M, NH-BARF 5.0  $\mu$ M (B/Re = 1.0), IP/Re = 2000 (except runs 13–16, see legend below). <sup>a</sup> Determined by gel permeation chromatography (GPC) against polystyrene standards. <sup>b</sup> Determined by <sup>1</sup>H and <sup>13</sup>C NMR spectra (numbers in parentheses determined by FT-IR). <sup>c</sup> Measured by differential scanning calorimetry (DSC). <sup>d</sup> IP/3 = 3000; <sup>e</sup> IP/3 = 4000; <sup>f</sup> IP/3 = 5000; <sup>g</sup> IP/3 = 10,000.

The microstructure of the PIR prepared from **1**- and **3**-NH-BARF consisted predominantly of the *cis*-1,4 head-to-tail repeating units (>98%) with occasional 3,4-inchainment, and no *trans*-1,4 unit existed. The *cis*-1,4 unit contents of PIR can be determined either by FT-IR or <sup>13</sup>C NMR spectroscopy [8–11], and both methods give highly comparable results, with negligible error of approximately 0.1–0.2% between the two (Table 1, data in parentheses are measured by FT-IR). Scheme 2 illustrates the carbon atoms numbering of isoprene monomer and the isomeric PIR macromolecule. Two representative <sup>13</sup>C NMR spectra of PIR samples are presented in Figure 2 with their chemical shifts. The *cis*-1,4, *trans*-1,4 and 3,4- isomeric units in the PIR macromolecule chains can be calculated according to Formulas (1)–(3), in which  $I_{23.46}$  is the integration of the *cis*-1,4-isoprene unit methyl carbon signal  $cC_5$  at 23.46 ppm,  $I_{18.64}$  is the integration of the 3,4-isoprene unit methyl carbon  $34C_5$  signal at 18.64 ppm, while  $I_{15.98}$  is the integration of the *trans*-1,4-isoprene unit methyl carbon  $tC_5$  signal at 15.98 ppm. Thus, For the PIR obtained from **1**- and **3**-NH-BARF in toluene, the molar percentage of the *cis*-1,4 and 3,4- isomeric unit is calculated using Formulas (1) and (3), respectively.

$$\text{Mol\% } cis\text{-1,4-IP\%} = [I_{23.46} / (I_{23.2} + I_{18.64} + I_{15.98})] \times 100\% \quad (1)$$

$$\text{Mol\% trans-1,4-IP\%} = [I_{15.98} / (I_{23.46} + I_{18.64} + I_{15.98})] \times 100\% \quad (2)$$

$$\text{Mol\% 3,4-IP\%} = [I_{18.64} / (I_{23.46} + I_{18.64} + I_{15.98})] \times 100\% \quad (3)$$



**Scheme 2.** Carbon atoms numbering in IP monomer and in different PIR macromolecular chains: (a) in IP monomer; (b) in *cis*-1,4 polymer [cPIR]; (c) in *trans*-1,4 polymer [tPIR]; (d) in 1,2-*isotactic* polymers [iPI12]; (e) in 3,4-*isotactic* polymers [iPI34]; (f) in 1,2-*syndiotactic* polymers [sPI12]; (g) in 3,4-*syndiotactic* polymers [sPI34].

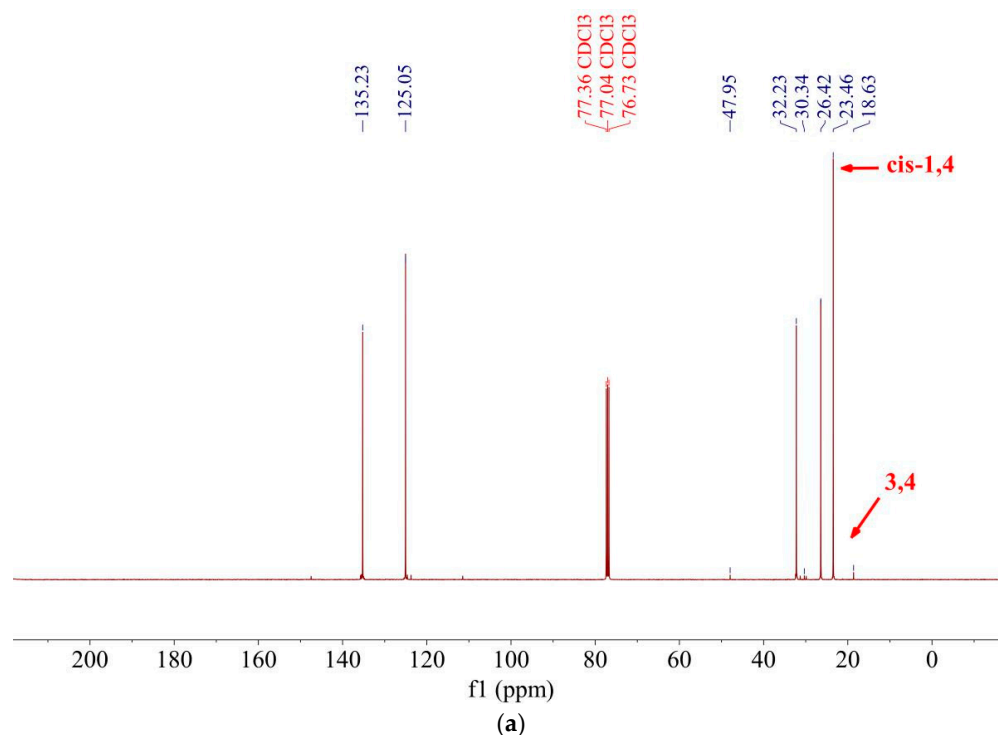


**Figure 2.** Cont.

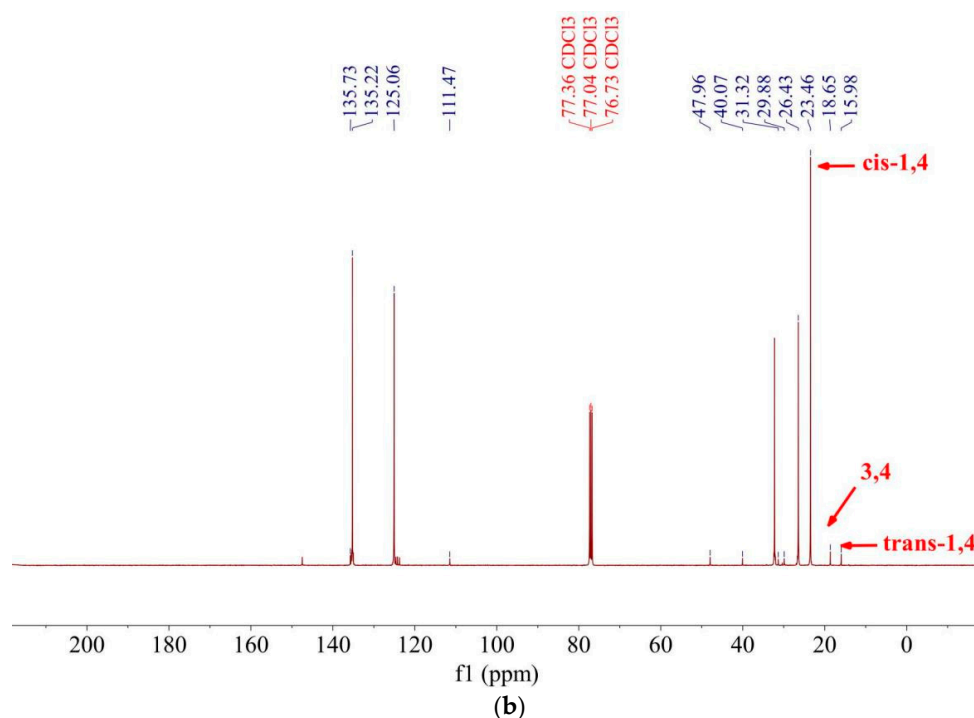


**Figure 2.** Representative  $^{13}\text{C}$  NMR spectra of PIR samples from toluene and hexane: (a)  $^{13}\text{C}$  NMR spectrum of PIR sample from toluene; (b)  $^{13}\text{C}$  NMR spectrum of PIR sample from hexane.

Polymerization temperature influenced sPIR molecular weight (Table 1, runs 3, 9–12) in a predictable way. PIR molecular weight increased near a linear manner with increasing  $T_p$  under incomplete monomer conversion, consistent with the quasi-living polymerization pattern (Figure 3a). At higher temperature conditions (40 °C and above), the PIR molecular weight reached maxima, due to an exhausted monomer. The molecular weight distribution was only marginally increased at higher temperatures.

Under the same reaction temperature and reaction time (20 °C, 30 min), gradually increasing the isoprene to catalyst ratio from 2000 to 10,000, the PIR molecular weight increased in a linear fashion, and the PIR microstructures were kept constant (Figure 3b, runs 13–16, 19)—evidence that has, again, pointed to the quasi-living polymerization mode. The relatively wide PIR molecular distributions from runs 16 and 19 (DPI 2.07 and 2.29, respectively) are most likely due to overrun the reaction after full monomer consumption, probably allowing the catalyst to rearrange the macromolecules in prolonged reaction times (*vide infra*). While for run 16, the high viscosity of high molecular weight PIR (Mw over 1300 kg/mol) caused reduced monomer diffusion to the catalyst center and the depleting monomer concentration in the late reaction stage, resulting in the reasons that widen the molecular distribution.

Catalyst efficiency was obviously dependent on the reaction time. The 1- and 3-NH-BARF catalytic systems showed rapid initiation and high catalytic efficiency above ambient temperature (turnover number, TON, about 920 IP/min at 40 °C, and TON above 1000 PI/min at 60 °C) with an effective catalyst of around 37% [18]. Figure 3c (runs 9, 3, 17–19) shows the reaction time dependence of PIR molecular weight and cis-1,4 content. Under the same reaction conditions ( $T_p$  = 20 °C and IP/3 = 2000), polymerization runs 3 and 17–19 all overrun the reaction under constant temperature, and the PIR microstructure experienced negligible influence by the reaction time (cis-1,4 content differences less than 0.1%); thus, extending the reaction time after monomer full consumption does not change the microstructure of PIR molecules, but surely alters the molecular weight in some degree and broadens the molecular weight distribution (*vide supra*).



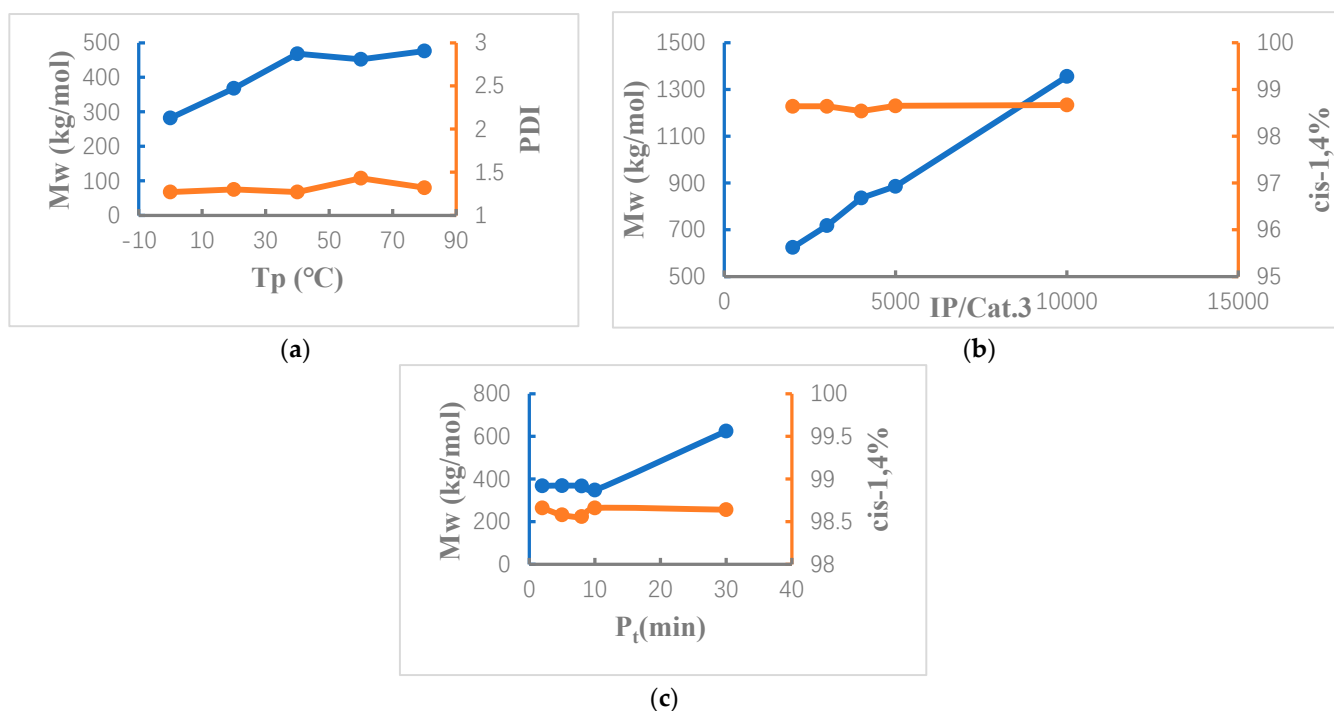


**Figure 3.** Polymerization temperature, IP/Re ratio and reaction time influence; (a) reaction temperature to Mw and DPI influence; (b) IP/3 ratio to Mw and stereoselectivity influence; (c) reaction time to Mw and stereoselectivity influence.

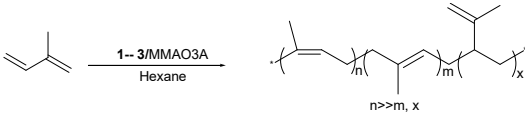
### 2.3. Polymerization of Isoprene with MMAO3A Activator in Hexane and Toluene

Aliphatic hydrocarbons are used in synthetic rubber (EPM/EPDM, PBR, SSBR, SBS, SEBS, etc.) production processes, and the catalysts or initiators involved in the production are either Ziegler, cationic or anionic type. The single site organometallic catalyst systems have the advantage of high activity, narrow molecular distribution, and easy microstructural manipulation. Owing to the cationic nature of most activated single-site organometallic catalysts, solubility is one of the obstacles to practical applications. The discovery of MAO is a great breakthrough for the application of organometallic catalysts in polyolefin industries [29–31], including MAO and the modified analogs applied to the synthetic rubber preparation [32,33].

Complexes 1–3, when combined with modified MAO—the commercially available MMAO3A—forms a soluble catalytic system that can initiate isoprene polymerization with a short induction time of approximately 5–10 min at low temperatures, while reaching to full monomer conversion in a few minutes at 80 °C (Table 2). Regarding factors of polymerization temperature, the reaction times suggested several points that are understood (*vide infra*). The 1-3-MMAO3A systems initiated polymerization in toluene with a shorter induction time of 2–3 min, but resulted in explicitly lower molecular weight sPIR (runs 11–14). The 3-MMAO3A catalytic system, in the absence of Al<sup>i</sup>Bu<sub>3</sub> (impurity scavenger), resulted in significantly higher molecular weight PIR (Mw 1163 kg/mol) with low monomer conversion (62%) within one hour, and broader molecular weight distribution (PDI 2.04, Table 2 run 4 *vide infra*).

Different from the NH-BARF activator, the catalyst 1-3-MMAO3A systems generated PIR macromolecular chains that contained high *cis*-1,4 isomeric units (91 to 95%) and non-ignorable amounts of *trans*-1,4 and 3,4- isomeric units (Table 2). The microstructure determined by <sup>13</sup>C NMR and FT-IR then had explicit differences, and the FT-IR method gave higher 1,4-isomeric unit contents.



**Table 2.** Polymerization of isoprene (IP) with complexes 1–3 and MMAO3A catalyst systems.


Run	Cat.	$P_t$ (min)	$T_p$ (°C)	Conversion %	Mw <sup>a</sup> (kg/mol)	PDI <sup>a</sup>	Microstructure <sup>b</sup>		
							<i>cis</i> -1,4%	<i>trans</i> -1,4%	3,4-cont.%
1	1	5	80	96	270	1.69	91.83 (97.60)	4.66	3.51
2	2	5	80	100	259	1.81	92.05 (97.39)	4.54	3.41
3	3	5	80	100	377	1.56	95.04 (97.73)	2.32	2.65
4	3	60	20	62	1163 <sup>d</sup>	2.04	95.12 (97.84)	2.04	2.84
5	3	60	20	85	598	1.58	94.74 (97.79)	2.37	2.89
6	3	20	40	99.7	354	1.66	93.73 (97.51)	3.14	3.14
7	3	30	40	100	401	2.12	94.44 (97.64)	2.78	2.78
8	3	10	80	100	428	2.10	94.81 (97.69)	2.57	2.63
9	3	120	0	100	240	1.78	94.15 (97.53)	2.96	2.89
10	3	180	0	100	313	1.75	93.99 (97.44)	3.04	2.97
11 <sup>c</sup>	3	60	0	93.2	225	1.77	(98.20)		
12 <sup>c</sup>	3	30	20	100	264	1.62	(98.13)		
13 <sup>c</sup>	3	30	40	100	181	1.92	(98.12)		
14 <sup>c</sup>	3	30	60	100	206	1.80	(98.10)		

Polymerization conditions: IP 1.0 M hexane solution 10 mL (10 mM),  $Al^iBu_3$ , 50  $\mu$ M, Re 5.0  $\mu$ M, MMAO3A 10 mM, IP/Re = 2000, Al/Re = 2050. <sup>a</sup> Determined by gel permeation chromatography (GPC) against polystyrene standards. <sup>b</sup> Determined by  $^1H$  NMR spectrum and  $^{13}C$  NMR spectrum, (number in parentheses determined by FT-IR). <sup>c</sup> Polymerization reaction carried out in toluene. <sup>d</sup> Polymerization without addition of  $Al^iBu_3$  (Al/Re = 2030) scavenger.

In the FT-IR spectrum of PIR,  $838\text{ cm}^{-1}$  was the *cis*-1,4 characteristic absorption band, the characteristic absorption band of 3,4-isomeric unit appeared at  $890\text{ cm}^{-1}$ , and the absorption band of *trans*-1,4 unit appeared at  $842\text{ cm}^{-1}$ . The deformation vibration absorption band of  $CH_3$  is at  $1357\text{ cm}^{-1}$ , and the bending vibration absorption band of the  $CH_2$  was at  $1454\text{ cm}^{-1}$ . The stretching vibration absorption band of  $C=C$  appeared at  $1654\text{ cm}^{-1}$  (see Supplementary Materials S1). Therefore, in FT-IR spectra, the low content *trans*-1,4 absorption band at  $842\text{ cm}^{-1}$  was usually merged into the tail of the strong *cis*-1,4 absorption band at  $838\text{ cm}^{-1}$ . Thus, the FT-IR method calculated the total 1,4 units against the 3,4 units using Formulas (4) and (5), in which  $A_{838}$  is the absorption band height of  $838\text{ cm}^{-1}$  ( $+842\text{ cm}^{-1}$ ), and  $A_{890}$  is the band height of 3,4-isomeric unit at  $890\text{ cm}^{-1}$  [8–11].

$$1,4\text{-isomeric units}\% = A_{838} / (A_{838} + A_{890}) \times 100\% \quad (4)$$

$$3,4\text{-isomeric units}\% = A_{890} / (A_{838} + A_{890}) \times 100\% \quad (5)$$

In contrast,  $^{13}C$  NMR spectra (Figure 2) clearly differentiates the *cis*-1,4 units methyl group ( $cC5$ , 23.42 ppm) with *trans*-1,4 unit methyl group ( $tC5$ , 15.98 ppm) and the 3,4 unit methyl group ( $_{34}C5$ , 18.64 ppm) chemical shifts. Comparing the sum of *cis*-1,4 and *trans*-1,4 units from  $^{13}C$  NMR integration with the FT-IR measured 1,4-isomeric unit content, the differences are in the range of +0.3% to +1.1%. Therefore, for the highly *cis*-1,4 and the predominantly *trans*-1,4 PIR macromolecular materials, FT-IR is a reliable method for the fast determination of the PIR microstructures [8,11].

For the complexes 1-, 2- and 3-MMAO3A catalytic systems in hexane, 3-MMAO3A showed better performance than the other two and gave PIR material with higher Mw and narrower DPI, but with lower reactivity. This is different from the NH-BARF-activated sys-

tems, in which complex **1** gave the highest molecular weight (777 kg/mol. vs. 369 kg/mol.) PIR with broader DPI (1.54 vs. 1.28. Table 1, run 1 vs. 3).

Temperature affected the **1**-, **2**- and **3**-MMAO3A catalytic systems in a different way (Figure 4). Polymerization at 20 °C gave the highest molecular weight PIR in both hexane and toluene, and the molecular weight attenuated with rising temperature to a minimum at around 40. The PIR molecular weight slightly increased (377 kg/mol vs. 428 kg/mol), accompanied with broadening DPI (1.56 vs. 2.10. Table 2. Run 3 vs. 8) after the IP monomer full conversion. A similar trend was found in the **3**-NH-BARF-activated system (*vide supra*).

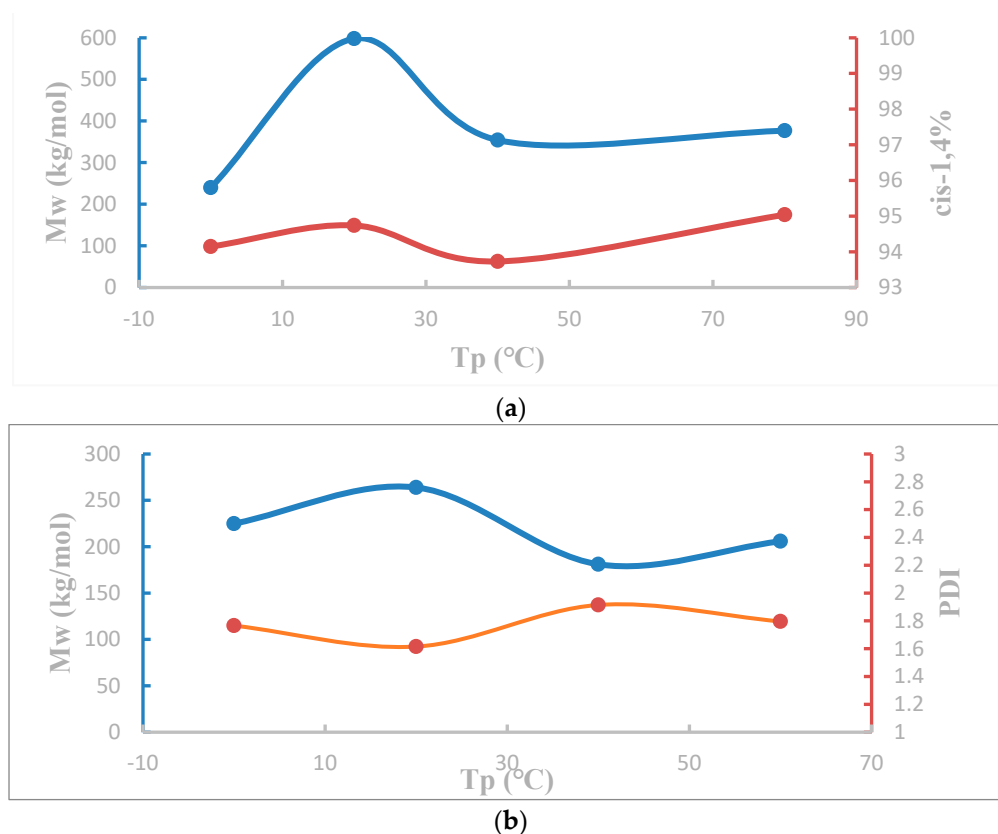


**Figure 4.** Influences of polymerization temperature on the molecular weight, molecular weight distribution and cis-1,4 content. (a) Temperature effect on Mw and cis-1,4 content for materials from **3**-MMAO3A in hexane; (b) temperature effect on Mw and DPI for materials from **3**-MMAO3A in toluene.

Interestingly, in the absence of the scavenger ( $\text{Al}^i\text{Bu}_3$ ), the polymerization reaction proceeded in a much slower speed due to a low level of effective catalyst (around 24% Table 2 run 3), whereas the effective catalyst was 36% (Table 2 run 4) in a similar reaction condition (20 °C, 60 min, IP/3 = 2000) in the existence of scavenger. Thus, the scavenger  $\text{Al}^i\text{Bu}_3$  was also serving as chain-transfer agent. Trialkylaluminum is widely used as an impurity scraper in the polyolefin industry [34], and it is also observed that trialkylaluminum bearing different alkyl substituent (for example Methyl, Ethyl, iso-Butyl, etc.) can switch the stereoselective pathway from the highly *cis*-1,4 PIR to the predominantly *isotactic*-3,4 microstructure resin in rare-earth metal catalyzed IP polymerization [35].

### 3. Discussion

The low catalyst effectivity in both activator-generated systems is most likely attributed to the low solubility of the cationic species in non-polar solvents (comparison of dielectric constant: toluene, 2.38; hexane, 2.05; chlorobenzene, 5.70) [36]. Complexes activated with NH-BARF in hexane appeared inactive, and the dielectric constant difference between the

two is not very large compared to the high polar solvent (such as chlorobenzene) used by the majority of researchers in cationic catalytic polymerization systems.

The phenomenon of increasing molecular weight accompanied with broadening molecular weight distributions after the IP monomer was exhausted in both activator system-initiated polymerization, is a familiar side reaction of catalytic redistributions, in which the rare-earth metal complexes can facilitate small molecules (for instance CO<sub>2</sub>) that are disproportionate [37], and a titanocene complex catalyzes small molecules of siloxane redistribution to form polysiloxanes [38].

The scavenger in the quasi-living polymerization system (Table 1) is most likely also playing a role of chain transfer [34], which leads to the reaction depart from the living pathway. It is expectable that well-balanced scavenging and chain-transferring actions in the polymerization [39] will offer better catalytic systems with higher catalytic efficiency and stereoselective capacity, which is a practical and worthwhile subject to be tackled.

#### 4. Materials and Methods

All synthetic procedures for the preparation of organorare-earth metal complexes and the experiments for polymerization of isoprene were carried out under standard Schlenk technique conditions. The vacuum-oven-dried Schlenk-type glassware was interfaced with a vacuum (10<sup>−5</sup> Torr) line; the vacuum/N<sub>2</sub> refilling circle with high purity N<sub>2</sub> (O<sub>2</sub> and H<sub>2</sub>O impurities level lower than 1.0 ppm) was repeated for three times prior to carrying out the synthetic/polymerization procedures, or the reactions were conducted in a high purity argon atmosphere double length glovebox (Vigor), in which the oxygen and moisture were kept below 0.1 ppm level.

Isoprene was purchased from Sinopharm Chemicals, and diluted with Toluene/hexane to a 1.0 M solution, adding triisobutylaluminum (TIBAL) 100 ppm (weight %) to react with the inhibitor, stored in a −20 °C refrigerator inside the glovebox for at least 48 h prior to use.

n-Butyllithium (1.0 M solution in n-hexane) was purchased from Sigma-Aldrich company and used as received. Chemicals and organic reagents for the synthesis of the tridentate PNP ligand were purchased from Sinopharm Chemicals, and were used as received. Bis(*o*-dipheylphosphinophenyl)amine, [(C<sub>6</sub>H<sub>5</sub>)<sub>2</sub>P-*o*-(C<sub>6</sub>H<sub>4</sub>)]<sub>2</sub>NH, was synthesized following the literature procedures [20]. Organic reagents and solvents were used as received in ordinary organic syntheses. The solvents used for preparing organorare-earth metal complexes were purified by passing through a serial column packed with molecular sieves (4A) and R3-11 catalyst (BASF), which kept the O<sub>2</sub> and moisture level lower than 1.0 ppm.

[PhMe<sub>2</sub>NH][B(C<sub>6</sub>F<sub>5</sub>)<sub>4</sub>] (99%) was purchased from Apalene Technology (Suzhou, China) and used as received. Anhydrous rare-earth metal trichlorides were purchased from Sigma-Aldrich, and were used as received.

Nuclear magnetic resonance (NMR) spectra for <sup>1</sup>H, <sup>13</sup>C and <sup>31</sup>P were recorded on a Bruker Avance 400 Ultrashield™ spectrometer (Bruker), and the chemical shifts were referenced with the deuterated solvent proton residual resonances, or the internal standard tetramethyl silane (TMS) signal. The deuterated NMR solvents were rigorously deoxygenated and demineralized when used for organorare-earth metal complex measurements.

Gel permeation chromatography (GPC) spectra were recorded on an Agilent 1260 Infinity II chromatogrammer, equipped with refractive index (RI), low angle laser light scattering (LALLS) and viscometry (VS) detectors. The columns were calibrated with polystyrene standards by use of the universal calibration methods [40–42]. All PIR samples were thoroughly dried in a vacuum oven under dynamic vacuum (ca. 50–100 Torr, 40 °C) to constant weight. The dried PIR samples (~10 Mg) were weighed out and dissolved in THF, and the solutions were passed through a 5 μm microfilter to remove insoluble species. GPC measurements were operated at 40 °C with THF eluent and an elution rate of 1.0 mL/min, and recorded with RI, LALLS and VS detectors.

Fourier transform infrared (FT-IR) spectra were recorded on a PerkinElmer Frontier (Perkin Elmer) Fourier transform infrared spectrometer. The PBR samples were prepared

using dried PBR row material and hot pressed into thin film, recorded with the transmission mode, scanning window  $4000\sim 400\text{ cm}^{-1}$ , and at least 36 cumulative scans. The spectra were stored in wave number ( $\text{cm}^{-1}$ ) and/or wave length ( $\lambda$ ) modes in a designated computer under specified file names for easy retrieving.

The glass-transition temperatures ( $T_g$ ) of PIR samples were recorded on a NATZSCH DSC 3500 Sirius differential Scanning Calorimeter. The PIR sample was cooled down to  $-140\text{ }^\circ\text{C}$  with a cooling rate of  $10\text{ }^\circ\text{C}/\text{min}$ , held for 5 min, and was then heated at rate of  $5\text{ }^\circ\text{C}/\text{min}$  to  $40\text{ }^\circ\text{C}$ . The midpoint of the glass transition temperature range was taken as the PIR's  $T_g$ .

The high-resolution mass spectroscopy (HR-MS) analysis was performed on a High-Resolution Orbitrap GC Mass Spectrometer (Q Exactive plus mass spectrometer. Thermo-Fisher Scientific, Germany) equipped with an electrospray ionization (ESI) source, and the air and moisture sensitive samples were handled following the literature methods [43,44].

Elemental analysis was performed on a UNICUBE elemental analyzer (Elementar, Langenselbold, Germany). Sample preparation, handling and injection, and other experimental conditions for C, H, N for the paramagnetic organometallic complexes analyses were adopted from operation manual of the equipment.

#### 4.1. Synthesis of Complexes 1, 2 and 3

The tridentate PNP ligand-supported rare-earth metal complexes,  $[(o\text{-Ph}_2\text{P-C}_6\text{H}_4)_2\text{N}]\text{Re}[(\text{CH}_2\text{-}o\text{-Me}_2\text{N}(\text{C}_6\text{H}_4))_2]$ : (Re = Y, **1**; Nd, **2**; Gd, **3**) were prepared following a modified literature procedure (Scheme 1) [20].

Complex **1**  $[(o\text{-Ph}_2\text{P-C}_6\text{H}_4)_2\text{N}]\text{Y}[(\text{CH}_2\text{-}o\text{-Me}_2\text{N}(\text{C}_6\text{H}_4))_2]$  preparation procedure: The PNP ligand  $[o\text{-Ph}_2\text{P}(\text{C}_6\text{H}_4)_2\text{NH}]$  (1.667 g, 3.10 mM), the tribenzyl complex  $\text{Y}(\text{CH}_2\text{-C}_6\text{H}_4\text{-}o\text{-NMe}_2)_3$  (1.475 g, 3.0 mM) and toluene 15 mL, in order, were added to a flame and vacuum dried flask containing a magnetic stirring bar. The mixture was stirred at an ambient temperature for 24 h. Toluene was evaporated under reduced pressure; the residual solid was taken up and washed with small portions of cold *n*-hexane (3 times); the residual yellow solid was dried under vacuum to a constant weight (2.31 g, Yield 86.2%).

The  $^1\text{H}$  and  $^{31}\text{P}$  NMR spectra of complex **1** are presented in Figure 1.  $^1\text{H}$  NMR (500 MHz,  $\text{C}_6\text{D}_6$ )  $\delta$  = 7.30 (m, 8H, Ar), 7.01 (m, 2H, Ar), 6.87 (m, 12H, Ar), 6.85 (m, 4H, Ar), 6.73 (d, 2H, Ar), 6.68 (m, 4H, Ar), 6.66 (m, 2H, Ar), 6.53 (t, 2H, Ar), 2.47 (s, 12H, 4CH<sub>3</sub>), 1.99 (s, 4H, 2CH<sub>2</sub>).

Complex **2**  $[(o\text{-Ph}_2\text{P-C}_6\text{H}_4)_2\text{N}]\text{Nd}[(\text{CH}_2\text{-}o\text{-Me}_2\text{N}(\text{C}_6\text{H}_4))_2]$  preparation follows the procedures as in complex **1**: The PNP ligand  $[o\text{-Ph}_2\text{P}(\text{C}_6\text{H}_4)_2\text{NH}]$  (1.70 g, 3.16 mM), the tribenzyl complex  $\text{Nd}(\text{CH}_2\text{-C}_6\text{H}_4\text{-}o\text{-NMe}_2)_3$  (1.69 g, 3.1 mM) and toluene 15 mL, in order, were added to a flame and vacuum dried flask containing a magnetic stirring bar. The mixture was stirred at an ambient temperature for 24 h. Toluene was evaporated under a reduced pressure; the residual solid was taken up and washed with small portions of cold *n*-hexane (3 times), the residual yellow solid was dried under vacuum to a constant weight (2.49 g, Yield 84.5%).

Complex **2** was analyzed with HR-MS (calculated molecular mass: 949.2165; measured molecular mass: 949.3028); and elemental analysis: (calculated elemental composition: C, 68.33%; H, 5.52%; P, 6.53%; N, 4.43%. Measured elemental composition: C, 68.12%; H, 5.38%; N, 4.26%).

Complex **3**  $[(o\text{-Ph}_2\text{P-C}_6\text{H}_4)_2\text{N}]\text{Gd}[(\text{CH}_2\text{-}o\text{-Me}_2\text{N}(\text{C}_6\text{H}_4))_2]$  preparation follows the procedures as in complex **2**: The PNP ligand  $[o\text{-Ph}_2\text{P}(\text{C}_6\text{H}_4)_2\text{NH}]$  (1.73 g, 3.21 mM), the tribenzyl complex  $\text{Gd}(\text{CH}_2\text{-C}_6\text{H}_4\text{-}o\text{-NMe}_2)_3$  (1.68 g, 3.0 mM) and toluene 15 mL, in order, were added to a flame and vacuum dried flask containing a magnetic stirring bar. The mixture was stirred at an ambient temperature for 24 h. Toluene was evaporated under a reduced pressure; the residual solid was taken up and washed with small portions of cold *n*-hexane (3 times), the residual yellow solid was dried under vacuum to a constant weight (2.47 g, Yield 85.6%).

Complex **3** was analyzed with HR-MS (calculated molecular mass: 962.2245; measured molecular mass: 962.3131); and elemental analysis: (calculated elemental composition: C, 67.41%; H, 5.45%; N, 4.37%; P, 6.44%. Measured elemental composition: C, 67.14%; H, 5.22%; N, 4.17%).

#### 4.2. Polymerizations in Toluene

A typical polymerization reaction in toluene was carried out in a glovebox under high purity argon atmosphere according to the following procedure.

Isoprene in toluene (1.0 M solution, 10 mL, 10.0 mM),  $\text{Al}(\text{iBu})_3$  (0.5 M solution in toluene, 0.5 mL, 0.25 mM,  $\text{Al}/\text{Re} = 50$ ), catalyst **3** (4.8 mg, 5.0  $\mu\text{M}$ ),  $[\text{PhMe}_2\text{NH}][\text{B}(\text{C}_6\text{F}_5)_4]$  (NH-BARF, 4.00 mg, 5.0  $\mu\text{M}$ ,  $\text{B}/\text{Re} = 1.0$ ), in order, were added to a Schlenk flask containing a magnetic stirring bar. The flask was merged in an oil bath at a designated temperature, and the mixture was stirred with a constant torque magnetic stirrer for an assigned time. The reaction was terminated by adding 0.5 mL of 2,6-di(*tert*-butyl)-4-methylphenol solution (0.1 M in toluene).

The flask was taken out of a glovebox, and the PIR was precipitated with ethanol, washed with deionized water (3 times), and then ethanol (2 times). The raw material was placed in a sample vial, dried in a vacuum oven under dynamic vacuum (50–100 torr, 40 °C) until a constant weight.

The polymerization reaction was repeated for at least two times to confirm the polymerization data accuracy.

In polymerization with higher IP/Re ratio (Table 1, runs 13–16), the same quantities of scavenger, catalyst **3**, activator were used, and a calculated amount of isoprene monomer solution was placed in the flask in the same order; the polymerization reactions were carried out at assigned conditions, and repeating experiments were performed accordingly.

#### 4.3. Polymerizations in Hexane

A typical polymerization reaction in hexane was carried out in a glovebox under high purity argon atmosphere according to the following procedure.

Isoprene in hexane (1.0 M solution, 10 mL, 10.0 mM),  $\text{Al}(\text{iBu})_3$  (0.5 M solution in hexane, 0.5 mL, 0.25 mM,  $\text{Al}/\text{Re} = 50$ ), catalyst **3** (4.8 mg, 5.00  $\mu\text{M}$ ), MMAO3A (0.60 g, 10 mM,  $\text{Al}/\text{Re} = 2000$ ), in order, were added to a Schlenk flask containing a magnetic stirring bar. The flask was merged in an oil bath at a designated temperature, and the mixture was stirred with a constant torque magnetic stirrer for an assigned time. The reaction was terminated by adding 1.0 mL of 2,6-di(*tert*-butyl)-4-methylphenol (0.5 M in toluene) and stirred for two minutes.

The flask was taken out of a glovebox, and the PIR was precipitated with ethanol (bubbles quickly evolving from the viscous solution when first few drops of ethanol added), washed with deionized water (3 times), and then ethanol (2 times). The raw material was placed in a sample vial, dried in a vacuum oven under dynamic vacuum (50–100 torr, 40 °C) until a constant weight.

The polymerization reaction was repeated for at least two times to confirm the polymerization results' accuracy.

**Supplementary Materials:** The following supporting information can be downloaded at: <https://www.mdpi.com/article/10.3390/catal12101131/s1>, **S1:** Representative FT-IR spectra for sPIR samples from complexes **1**-, **3**-NH-BARF catalyst system polymerization runs 4–19 in Table 1; **S2:** Representative C-13 NMR spectra for sPIR samples from complexes **1**-, **3**-NH-BARF catalyst system, polymerization runs 4–19 in Table 1; **S3:** Representative GPC plots for sPIR samples from complexes **1**-, **3**-NH-BARF catalyst system, polymerization runs 4–19 in Table 1; **S4:** Representative DSC diagrams for sPIR samples from complexes **1**-, **3**-NH-BARF catalyst system, polymerization runs 5 and 18 in Table 1; **S5:** Representative C-13 NMR spectra for sPIR samples from complexes **1**-**3**-MMAO3A catalyst system, polymerization runs in Table 2; **S6:** Representative GPC plots for sPIR samples from complexes **1**-**3**-MMAO3A catalyst system, polymerization runs in Table 2.



**Author Contributions:** R.M. (candidate) complexes syntheses and polymerization reactions; H.H. mentor; X.L. and Y.Z. daily advisory; X.S. and H.L. project administration; X.Z. analytical data acquisition; G.M. mentor and methodology; S.X. funding acquisition, supervision, writing—review and editing. All authors have read and agreed to the published version of the manuscript.

**Funding:** This research was funded by the Natural Science Foundation of China through project number 22172024.

**Acknowledgments:** The authors appreciated the help of the Advanced Material Research Institute of Shandong Jincheng Petrochemical Group in help of measuring of most GPC, DSC, and NMR data acquisition and analyses.

**Conflicts of Interest:** The authors declare no conflict of interest. The funders had no role in the design of the study; in the collection, analyses, or interpretation of data; in the writing of the manuscript; or in the decision to publish the results.

## References

- Senysek, M.L. Isoprene Polymers. In *Encyclopedia of Polymer Science and Technology*, 4th ed.; Herman, M.F., Ed.; John Wiley & Sons Inc.: New York, NY, USA, 2014; Volume 7, pp. 270–348.
- Takeuchi, D. Stereoselective Polymerization of Conjugated Dienes. In *Encyclopedia of Polymer Science and Technology*, 4th ed.; Herman, M.F., Ed.; John Wiley & Sons Inc.: New York, NY, USA, 2014; Volume 13, pp. 126–150.
- Ricci, G.; Sommazzi, A.; Masi, F.; Ricci, M.; Boglia, A.; Leone, G. Well-defined transition metal complexes with phosphorus and nitrogen ligands for 1,3-dienes polymerization. *Coord. Chem. Rev.* **2010**, *254*, 661–676. [\[CrossRef\]](#)
- Puskas, J.E.; Gautriaud, E.; Deffieux, A.; Kennedy, J.P. Natural rubber biosynthesis—A living carbocationic polymerization. *Prog. Polym. Sci.* **2006**, *3*, 533–548. [\[CrossRef\]](#)
- Ouardad, S.; Deffieux, A.; Peruch, F. Polyisoprene synthesized via cationic polymerization: State of the art. *Pure Appl. Chem.* **2012**, *84*, 2065–2080. [\[CrossRef\]](#)
- Zhang, S.; Wu, N.; Wu, Y.X. Highly *Cis*-1,4 Selective Polymerization of Conjugated Dienes Catalyzed by *N*-heterocyclic Carbene-ligated Neodymium Complexes. *Chin. J. Polym. Sci.* **2020**, *38*, 1305–1312. [\[CrossRef\]](#)
- Guo, G.; Wu, X.L.; Yan, X.Q.; Yan, L.; Li, X.F.; Zhang, S.W.; Qiu, N.N. Unprecedentedly High Activity and/or High Regio-/Stereoselectivity of Fluorenyl-Based CGC Allyl-Type  $\eta^3$ : $\eta^1$ -*tert*-Butyl(dimethylfluorenylsilyl)amido Ligated Rare Earth Metal Monoalkyl Complexes in Olefin Polymerization. *Polymer* **2019**, *11*, 836. [\[CrossRef\]](#)
- Tan, J.M.; Li, C.Q.; Xu, L.; Zhang, J.; Liang, A.M.; Zhang, L.Q.; Wu, S.Z. Study on the Microsequence Structure and Crystallization Properties of Isoprene Rubber. *Sci. Sin. Chim.* **2014**, *44*, 1733–1739.
- Tanaka, Y.; Sato, H. Sequence distribution of polyisoprenes. *Polymer* **1976**, *17*, 413–418. [\[CrossRef\]](#)
- Sato, H.; Ono, A.; Tanaka, Y. Distribution of isomeric structures in polyisoprenes. *Polymer* **1977**, *18*, 580–586. [\[CrossRef\]](#)
- Tuampoemsab, S.; Nimpaboon, A.; Sakdapipanich, J.T. Quantitative analysis of isoprene units in natural rubber and synthetic polyisoprene using  $^1\text{H}$ -NMR spectroscopy with an internal standard. *Polym. Test.* **2015**, *43*, 21–26. [\[CrossRef\]](#)
- FMI. Synthetic Polyisoprene Market Size, Industry Share & Trends–2032. Available online: <https://www.futuremarketinsights.com/reports/synthetic-polyisoprene-rubber-market> (accessed on 22 July 2022).
- Chen, W.Q.; Wang, F.S. Synthetic rubbers prepared by lanthanide coordination catalysts. *Sci. China B Chem.* **2009**, *52*, 1520–1543. [\[CrossRef\]](#)
- Zhang, Z.C.; Cui, D.M.; Wang, B.L.; Liu, B.; Yang, Y. Polymerization of 1,3-conjugated dienes with rare-earth metal precursors. In *Structure and Bonding, Molecular Catalysis of Rare-Earth Elements*; Mingos, D.M.P., Roesky, P.W., Eds.; Springer: Berlin, Germany, 2010; Volume 137, pp. 49–108.
- Hou, Z.M.; Suzuki, T. Scandium and yttrium complexes for well-controlled polymerization. *Mater. Integr.* **2007**, *21*, 34–42.
- Shen, Z.Q. Catalytic activities of rare-earth calixarene complexes in polymer syntheses. *Chin. J. Polym. Sci.* **2005**, *23*, 593–602. [\[CrossRef\]](#)
- Zhang, G.C.; Deng, B.J.; Wang, S.W.; Wei, Y.; Zhou, S.L.; Zhu, X.C.; Huang, Z.M.; Mu, X.L. Di and trinuclear rare-earth metal complexes supported by 3-amido appended indolyl ligands: Synthesis, characterization and catalytic activity towards isoprene 1,4-*cis* polymerization. *Dalton Trans.* **2016**, *45*, 15445–15456. [\[CrossRef\]](#) [\[PubMed\]](#)
- Zhang, L.X.; Suzuki, T.; Luo, Y.; Nishiura, M.; Hou, Z.M. Cationic Alkyl Rare-Earth Metal Complexes Bearing an Ancillary Bis(phosphinophenyl)amido Ligand: A Catalytic System for Living *cis*-1,4-Polymerization and Copolymerization of Isoprene and Butadiene. *Angew. Chem. Int. Ed.* **2007**, *46*, 1909–1913. [\[CrossRef\]](#) [\[PubMed\]](#)
- Nishiura, M.; Hou, Z.M. Novel polymerization catalysts and hydride clusters from rare-earth metal dialkyls. *Nat. Chem.* **2010**, *2*, 257–268. [\[CrossRef\]](#)
- Suzuki, T.; Zhang, L.X.; Hou, Z.M. Metal Complex Containing Tridentate Ligand, and Polymerization Catalyst Comprising the Same. U.S. Patent Application 11/795,571, 15 May 2008.

21. Friebe, L.; Nuyken, O.; Obrecht, W. Neodymium-Based Ziegler/Natta Catalysts and Their Application in Diene Polymerization. In *Neodymium Based Ziegler Catalysts—Fundamental Chemistry*; Nuyken, O., Ed.; Springer: Berlin/Heidelberg, Germany, 2006; Volume 204, pp. 1–154.
22. Ren, W.H.; Liu, H.; You, F.; Mao, P.J.; So, Y.M.; Kang, X.H.; Shi, X.C. Unsymmetrical diarylamido-based rare-earth alkyl complexes: Their synthesis and catalytic performance in isoprene polymerization. *Dalton Trans.* **2021**, *50*, 1334–1343. [\[CrossRef\]](#)
23. Yu, C.; Zhou, D.H.; Yan, X.Q.; Gao, F.; Zhang, L.; Zhang, S.W.; Li, X.F. Cis-1,4-polymerization of isoprene by 1,3-bis(oxazolinymethylidene)isoindoline-ligated rare-earth metal dialkyl complexes. *Polymer* **2017**, *9*, 531. [\[CrossRef\]](#) [\[PubMed\]](#)
24. Basalova, O.A.; Tolpygin, A.O.; Kovylina, T.A.; Cherkasov, A.V.; Fukin, G.K.; Trifonov, A.A. Bis(tetramethylaluminate) rare-earth metal Complexes Supported by Bi- and Tridentate Amidinate Ligands: Performance in Isoprene Polymerization. *Organometallic* **2021**, *40*, 979–988. [\[CrossRef\]](#)
25. Zhang, P.F.; Liao, H.Y.; Wang, H.H.; Li, X.F.; Yang, F.Z.; Zhang, S.W. Cis-1,4-Polymerization of Isoprene Catalyzed by 1,3-Bis(2-pyridylimino)isoindoline-Ligated Rare-Earth-Metal Dialkyl Complexes. *Organometallic* **2017**, *36*, 2446–2451. [\[CrossRef\]](#)
26. Pan, Y.; Li, W.Q.; Wei, N.N.; So, Y.M.; Li, Y.; Jiang, K.; He, G.H. Anilido-oxazoline-ligated rare-earth metal complexes: Synthesis, characterization and highly cis-1,4-selective polymerization of isoprene. *Dalton Trans.* **2019**, *48*, 3583–3592. [\[CrossRef\]](#)
27. Trifonov, A.A.; Lyubov, D.M.A. Quarter-century long story of bis(alkyl) rare-earth (III) complexes. *Coord. Chem. Rev.* **2017**, *340*, 10–61. [\[CrossRef\]](#)
28. Zhang, L.X.; Hou, Z.M. Unprecedented Isospecific 3,4-Polymerization of Isoprene by Cationic Rare-Earth Metal Alkyl Species Resulting from a Binuclear Precursor. *J. Am. Chem. Soc.* **2005**, *127*, 14562–14563. [\[CrossRef\]](#) [\[PubMed\]](#)
29. Andersen, A.; Cordes, H.G.; Herwig, H.; Kaminsky, W.; Merk, A.; Mottweiler, R.; Pein, J.; Sinn, H.; Vollmer, H.J. Halogen-Free Soluble Ziegler catalysts for the polymerization of Ethylene, Control of Molecular Weight by Choice of Temperature. *Angew. Chem. Int. Ed. Engl.* **1976**, *15*, 630–632. [\[CrossRef\]](#)
30. Resconi, L.; Covallo, L.; Fait, A.; Piemontes, F. Selectivity in Propene Polymerization with Metallocene Catalysts. *Chem. Rev.* **2000**, *100*, 1253–1345. [\[CrossRef\]](#)
31. Alt, H.G.; Koppl, A. Effect of the Nature of Metallocene Complexes of Group IV Metals on Their Performance in Catalytic Ethylene and propylene Polymerization. *Chem. Rev.* **2000**, *100*, 1205–1221. [\[CrossRef\]](#) [\[PubMed\]](#)
32. Kaminsky, W. New Elastomers by Metallocene Catalysis. *Macromol. Symp.* **2001**, *174*, 269–276. [\[CrossRef\]](#)
33. Luconi, L.; Lyubov, D.M.; Rossin, A.; Glukhova, T.A.; Cherkasov, A.V.; Tuci, G.; Fukin, G.K.; Trifonov, A.A.; Giambastiani, G. Organolanthanide complexes supported by thiazole-containing amidopyridinate ligands: Synthesis, characterization, and catalytic activity in isoprene polymerization. *Organometallic* **2014**, *33*, 7125–7134. [\[CrossRef\]](#)
34. Bruaseth, I.; Rytte, E. Dual Site Ethene/1-Hexene Copolymerization with MAO Activated (1,2,4-Me<sub>3</sub>Cp)<sub>2</sub>ZrCl<sub>2</sub> and (Me<sub>5</sub>Cp)<sub>2</sub>ZrCl<sub>2</sub> Catalysts. Possible Transfer of Polymer Chains between the Sites. *Macromolecules* **2003**, *36*, 3026–3034. [\[CrossRef\]](#)
35. Zhang, L.X.; Nishiura, M.; Yuki, M.; Luo, Y.; Hou, Z.M. Isoprene Polymerization with Yttrium Amidinate Catalysts: Switching the Regio- and Stereoselectivity by Addition of AlMe<sub>3</sub>. *Angew. Chem. Int. Ed.* **2008**, *47*, 2642–2645. [\[CrossRef\]](#)
36. The Engineering Toolbox. Liquids Dielectric Constants. Available online: <https://www.engineeringtoolbox.com> (accessed on 29 July 2022).
37. Davies, N.W.; Frey, A.S.P.; Gardiner, M.G.; Wang, J. Reductive disproportionation of carbon dioxide by a Sm(II) complex: Unprecedented f-block element reactivity giving a carbonate complex. *Chem. Commun.* **2006**, *46*, 4853–4855. [\[CrossRef\]](#)
38. Xin, S.X.; Aitken, C.; Harrod, J.F.; Mu, Y.; Samuel, E. Redistribution Reactions of Alkoxy- and Siloxysilanes, Catalyzed by Dimethyltitanocene. *Can. J. Chem.* **1990**, *68*, 471–476. [\[CrossRef\]](#)
39. Fink, G.; Steinmetz, B.; Zechlin, J.; Przybyla, C.; Tesche, B. Propene Polymerization with Silica-Supported Metallocene/MAO Catalysts. *Chem. Rev.* **2000**, *100*, 1377–1390. [\[CrossRef\]](#) [\[PubMed\]](#)
40. Dunkai, N.; Nakazawa, A.; Inagaki, H. A Universal Calibration in Gel Permeation Chromatography. *Bull. Inst. Chem. Res. Kyoto Univ.* **1970**, *48*, 79–87.
41. Dawkins, J.V. Calibration Procedures in Gel Permeation Chromatography. *Br. Polym. J.* **1972**, *4*, 87–101. [\[CrossRef\]](#)
42. Crouzet, P.; Martens, P.; Mangin, P. Universal Calibration in Permeation Chromatography. Application to Polyethylene, Polypropylene, and Ethylene-Propylene Copolymers. *J. Chromatogr. Sci.* **1971**, *9*, 525–530. [\[CrossRef\]](#)
43. Dyson, P.J.; McIndoe, J.S. Analysis of organometallic compounds using ion trap mass spectrometry. *Inorg. Chim. Acta* **2003**, *354*, 68–74. [\[CrossRef\]](#)
44. Johnstone, R.A.W.; Cragg, R.H. Organometallic, co-ordination, and inorganic compounds investigated by mass spectrometry Mass Spectrometry. In *Mass Spectrometry of Inorganic and Organometallic Compounds*; Hendersen, W., McIndoe, J.S., Eds.; Wiley: New York, NY, USA, 2005; Volume 6, pp. 294–328.